Kinetics-free transformation from non-isothermal discontinuous to continuous tubular reactors

Federico Florit[a], Valentina Busini[a], Giuseppe Storti[b], Renato Rota[a,*]

[a] *Politecnico di Milano, Dipartimento di Chimica, Materiali e Ingegneria Chimica G. Natta, via Mancinelli 7, 20131, Milano, Italy*
[b] *ETH Zürich, Department of Chemistry and Applied Biosciences, Vladimir-Prelog-Weg 1-5/10, HCI F 125, 8093 Zürich, Switzerland*

Abstract

Focusing on tubular reactors with continuously distributed side injections, a general procedure to evaluate the operating mode able to reproduce the performance of a given semi-batch reactor is worked out. Namely, such operating mode is expressed as axial profiles of feed flowrate and temperature of the cooling/heating medium inside the reactor jacket. This transformation procedure, previously limited to isothermal reactors, is extended here to non-isothermal systems. The process performance (selectivity and conversion) of the original discontinuous reactor are fully reproduced using the continuous intensified reactor, while its productivity remains a degree of freedom. Notably, like in the isothermal case, the transformation procedure is kinetics-free, i.e. the knowledge of the reaction kinetics is not a precondition.

As case study, a copolymerisation reaction is considered to demonstrate the potential of the method. Even though any SBR feed policy could be considered when applying this methodology, the optimal feed policy of the semi-batch reactor evaluated according to the so-called "power feed" procedure is examined considering the reactor non-isothermal. Afterwards, the proposed transformation method is applied and the performance of the two systems, discontinuous and continuous, are comparatively evaluated. Finally, given the practical difficulties associated with continuously distributed side injections, a discretisation approach is proposed based on the use of discrete lateral feeds and more realistic reactor configurations.

Keywords: Semi-batch to continuous, Process Intensification, Kinetics-free, Tubular reactor

1. Introduction

As part of a general framework focused on safety and production enhancement of existing processes, the transformation of discontinuous processes into continuous ones is a trending topic of process intensification as

*Corresponding author
Email address: renato.rota@polimi.it (Renato Rota)

well as the so-called flow chemistry [1, 2]. The transition to continuous processes offers several advantages, such as a more effective temperature control [3]. In particular, thermal runaway is one major concern in discontinuous processes when exothermic reactions are involved [4] and can be more easily handled in continuous processes, where higher cooling capacity reactors can be exploited, e.g., using tubular heat-exchanger-like reactors [5, 6]. This way, hazardous chemical reactions can be run using operating conditions (e.g., temperature, pressure, reactant concentrations) which would lead to a loss of control in discontinuous reactors, therefore improving the plant productivity. Secondly, smaller size reactors can be used at constant production rate because of the reduction of reactor hold-up typically encountered in continuous operations [7], with a substantial increase of intrinsic safety. Finally, larger reproducibility of the product properties can be achieved, given the improved quality control typically associated with continuous feed flowrates in contrast to discontinuous processes [8].

A popular example of products associated with reactions almost invariably carried out in batch (BR) or semi-batch reactors (SBR) are the polymer materials. Given the huge market demand of plastics, optimal operating modes (or recipes) are available for these reactors. For example, *ad hoc* temperature profiles in time were determined for polymerisations carried out in BRs to achieve given product features in minimum time [9]. SBRs can also be optimised with respect to product quality by tuning the feed policy and/or the operating temperature in time. In this case, the so-called "power feed" policy for the control of the product composition in copolymerisation represents a paradigm, which enables given quality features in much shorter times compared to industrially popular techniques like the "starved feed" policy [10, 11]. Such extent of optimisation is actually hindering the transformation of these processes into continuous ones, since the need to keep at least the same quality of the original (fully optimised) discontinuous process is a necessary condition.

In a previous work [12], we demonstrated how an isothermal SBR-based process can be carried out continuously using a tubular reactor with lateral injections (Lateral Injection Reactor, LIR) operated under isothermal conditions. Always assuming ideal type reactors (perfect mixing inside the SBR, plug flow in the tubular reactor), this special type of reactor can be regarded as a Zwietering-like tubular reactor [13]. Through this approach, the developed continuous process reproduces conversion and selectivity axial profiles identical to those established in time inside the SBR, but with the advantage of retaining the productivity as a degree of freedom. Therefore, using the LIR allows for keeping the same product quality while increasing the productivity.

Since the temperature profile can influence the process performance significantly, the aim of this work is

to extend the transformation procedure to non-isothermal SBR processes (based on optimised recipes) using LIRs. After the development of the general theoretical framework, the approach will be verified through a case study focused on a copolymerisation reaction with composition control. In particular, the optimal feed policy of the SBR evaluated according to the so-called "power feed" procedure will be examined, considering non-isothermal reactor. Finally, another reactor configuration will be explored in the continuous case as a more practical implementation of the ideal LIR.

2. Model formulation

Let us consider an industrial non-isothermal reaction carried out in liquid phase inside an ideal SBR following a well-established recipe. The schematic representation of this reactor is shown in Figure 1, where an initial charge with given quantity of each component, $m^*_{i,0}$ $(i = 1, \ldots, NC)$, is assumed. The different species are added in time according to defined mass flowrates, $F^*_i(t)$, while the temperature profile is tuned by suitable time-variable heat flow through the reactor wall, $\dot{Q}^*(t)$. Our aim is the transformation of such discontinuous process into a continuous one while reproducing the original SBR performance in terms of conversion and selectivity. As continuous reactor, we will consider a LIR, the tubular reactor with continuous lateral specific mass flowrates for each species, $f_i(x)$, shown in Figure 2. In the same figure, $\dot{q}(x)$ represents the axial profile of heat flow exchanged through the reactor wall using a cooling/heating medium flowing inside the reactor jacket.

2.1. SBR equations

The considered SBR model is made of overall and species mass balance equations, an equation of state (as discussed in detail elsewhere [12]), and the energy balance equation, together with the corresponding initial conditions. According to the assumption of ideal reactors, the reacting mixture is well mixed, i.e., with uniform properties over the entire reactor volume.

Species mass balance equations can be written as:

$$\frac{d\omega^*_i}{dt} = \frac{F^*_i(t)}{m^*} - \omega^*_i \frac{F^*(t)}{m^*} + \frac{\dot{\Omega}_i(\underline{\omega}^*, T^*)}{\rho^*(t)} \tag{1}$$

where ω^*_i is the mass fraction of species i in the SBR, F^*_i the feedrate of species i, t the time, m^* the total mass inside the reactor, $\dot{\Omega}_i$ the species i mass production rate, T^* the temperature, and ρ^* the density of the reacting mixture. Note that an asterisk has been added as superscript to some variables to highlight

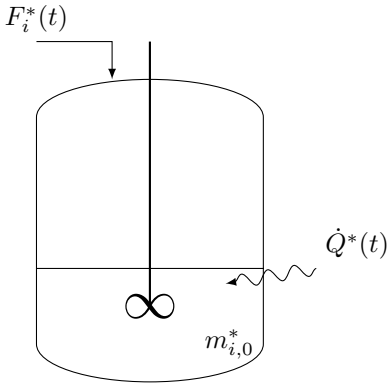

Figure 1: Semi-batch reactor. $m_{i,0}^*$[kg] is the initially charged amount of species i, $F_i^*(t)$[kg s^{-1}] the feed rate of species i, $\dot{Q}^*(t)$[W] the heat flux at the heat exchange surface.

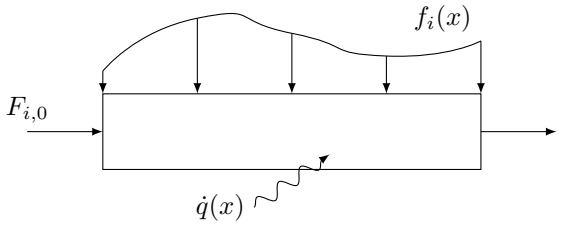

Figure 2: Tubular reactor with continuous lateral injections. $F_{i,0}$[kg s^{-1}] is the inlet flow rate of species i, $f_i(x)$[kg m^{-1} s^{-1}] the specific side feed rate of species i per unit length of the reactor, $\dot{q}(x)$[W m^{-1}] the specific heat flux per unit length at the exchange surface.

their belonging to the SBR; note also that some notation is slightly changed with respect to [12].

The overall mass balance equation is:

$$\frac{dm^*}{dt} = F^*(t) \tag{2}$$

where

$$F^*(t) \stackrel{\text{def}}{=} \sum_{i=1}^{NC} F_i^*(t) \tag{3}$$

The corresponding initial conditions for species and overall mass balance equations are respectively:

$$\omega_i^*(0) = \frac{m_{i,0}^*}{m_0^*} \tag{4}$$

$$m^*(0) = m_0^* \tag{5}$$

Density is given by an equation of state as a function of composition and temperature (and therefore time), generally expressed as:

$$\rho^*(t) = \rho(\underline{\omega}^*(t), T^*(t)) \tag{6}$$

Of course, $\rho^* = \text{const}$ corresponds to the simplest case.

The energy balance can be expressed in terms of enthalpy:

$$\frac{dH^*}{dt} = \dot{H}^{F^*} + \dot{Q}^*(t) \tag{7}$$

where H^* is the total enthalpy, $\dot{H}^{F^*}$ the enthalpy flow associated with the feed flowrate, and $\dot{Q}^*(t)$ the total heat flow through the reactor wall. Using partial molar quantities, such total enthalpies can be expressed as:

$$H^* = \sum_{i=1}^{NC} \overline{H}_i^* \frac{m_i^*}{MW_i} \tag{8}$$

$$\dot{H}^{F^*} = \sum_{i=1}^{NC} \overline{H}_i^{F^*} \frac{F_i^*}{MW_i} \tag{9}$$

where $\overline{H}_i^*$ and $\overline{H}_i^{F^*}$ are the partial molar enthalpies of species i evaluated at reactor and feed conditions, respectively, while MW_i is the molecular weight of species i. Combining the material balances (1) with the energy balance (9), the following final form of the energy balance for the SBR is worked out:

$$m^* c_p^*(t) \frac{dT^*}{dt} = \sum_{i=1}^{NC} \frac{F_i^*}{MW_i} (\overline{H}_i^{F^*} - \overline{H}_i^*) - \frac{m^*}{\rho^*} \sum_{j=1}^{NR} \Delta H_{R,j}(T^*) r_j(\underline{\omega}^*, T^*) + \dot{Q}^*(t) \tag{10}$$

where c_p^* is the mass-specific heat capacity of the reacting mixture, $\Delta H_{R,j}$ the j-th reaction enthalpy ($j = 1 \dots NR$), and r_j the j-th molar reaction rate. The initial condition for the last previous equation is:

$$T^*(0) = T_0^* \tag{11}$$

To evaluate the additional properties associated with the energy balance (specific heat capacities and partial molar enthalpies of reacting mixture and feed), suitable thermodynamic equations are needed, here generically represented by the functional forms below:

$$c_p^*(t) = c_p^*(\underline{\omega}^*(t), T^*(t)) \tag{12}$$

$$\overline{H}_i^*(t) = \overline{H}_i^*(\underline{\omega}^*(t), T^*(t)) \tag{13}$$

$$\overline{H}_i^{F^*}(t) = \overline{H}_i^{F^*}(\underline{\omega}^{F^*}(t), T_{F^*}(t)) \tag{14}$$

where $\omega_i^{F^*} = F_i^*/F^*$ is the feed composition and T_F the feed temperature.
In the simplest case of ideal mixtures, partial molar enthalpy coincides with specific molar enthalpy. Assuming also constant heat capacity of each component, the final energy balance equation simplifies to:

$$m^* \left(\sum_{i=1}^{NC} \omega_i^* c_{p,i} \right) \frac{dT^*}{dt} = \left(\sum_{i=1}^{NC} F_i^* c_{p,i} \right) (T_{F^*} - T^*) - \frac{m^*}{\rho^*} \sum_{j=1}^{NR} \Delta H_{R,j}(T^*) r_j(\underline{\omega}^*, T^*) + \dot{Q}^* \tag{15}$$

where $c_{p,i}$ is the mass-specific heat capacity of species i.

2.2. LIR equations

Similarly, mass and energy balance equations can be written for the considered continuous reactor. Under the assumption of plug flow, species mass balance equations are:

$$\frac{d\omega_i}{dx} = \frac{1}{F(x)} \Big(f_i(x) - \omega_i f(x) + \dot{\Omega}_i(\underline{\omega}, T) \mathscr{A}(x) \Big) \tag{16}$$

where ω_i is the species i mass fraction in the tubular reactor, x the axial coordinate, $f_i(x)$ the continuous specific lateral feed flowrate of species i, F the total mass flowrate, T the temperature, $\mathscr{A}$ the cross sectional area, and $f(x)$ is defined as:

$$f(x) \stackrel{\text{def}}{=} \sum_{i=1}^{NC} f_i(x) \tag{17}$$

The overall mass balance equation becomes:

$$\frac{dF}{dx} = f(x) \tag{18}$$

Boundary conditions for these equations are:

$$\omega_i(0) = \omega_{i,0} \tag{19}$$

$$F(0) = F_0 \tag{20}$$

where F_0 and $\omega_{i,0}$ are the inlet mass flowrate and mass fraction of species i, respectively.

Again, an equation of state is required to evaluate the mixture density, generically expressed as a function of mixture composition and temperature as below:

$$\rho(x) = \rho(\underline{\omega}(x), T(x)) \tag{21}$$

being $\rho = \text{const}$ the simplest case.

Moving now to the energy balance, for an open system at steady state we can consider the following enthalpy balance:

$$\frac{d\dot{H}}{dx} = \dot{H}^f + \dot{q} \tag{22}$$

where $\dot{H}$ is the total enthalpy flow, $\dot{H}^f$ the length-specific enthalpy flow, and $\dot{q}$ the length-specific heat flow exchanged through the reactor wall. In terms of partial molar quantities, the total enthalpy flows can be expressed as:

$$\dot{H} = \sum_{i=1}^{NC} \overline{H}_i \frac{F_i}{MW_i} \tag{23}$$

$$\dot{H}^f = \sum_{i=1}^{NC} \overline{H}_i^f \frac{f_i}{MW_i} \tag{24}$$

where $\overline{H}_i$ and $\overline{H}_i^f$ are the partial molar enthalpies of species i as a function of the axial position inside the tubular reactor and of the lateral feed, respectively. Exploiting Equation (16), the energy balance equation becomes:

$$Fc_p(x)\frac{dT}{dx} = \sum_{i=1}^{NC} \frac{f_i}{MW_i}(\overline{H}_i^f - \overline{H}_i) - \mathscr{A}\sum_{j=1}^{NR} \Delta H_{R,j}(T) r_j(\underline{\omega}, T) + \dot{q} \tag{25}$$

with the initial condition:

$$T(0) = T_0 \tag{26}$$

Once more, to evaluate the specific heat capacities and the partial molar enthalpies of reacting mixture and feed, suitable thermodynamic equations are needed, here generically represented by the functional forms below:

$$c_p(x) = c_p(\underline{\omega}(x), T(x)) \tag{27}$$

$$\overline{H}_i(x) = \overline{H}_i(\underline{\omega}(x), T(x)) \tag{28}$$

$$\overline{H}_i^f(x) = \overline{H}_i^f(\underline{\omega}^f(x), T_f(x)) \tag{29}$$

where $\omega_i^f = f_i/f$ is the feed composition and T_f the feed temperature.

For ideal mixtures and assuming constant specific heats, the simplified form of the enthalpy balance equation is:

$$F\left(\sum_{i=1}^{NC}\omega_i c_{p,i}\right)\frac{dT}{dx} = \left(\sum_{i=1}^{NC} f_i c_{p,i}\right)(T_f - T) - \mathscr{A}\sum_{j=1}^{NR}\Delta H_{R,j}(T) r_j(\underline{\omega}, T) + \dot{q} \tag{30}$$

Finally, the new quantity elapsed time, $\theta(x)$, is conveniently introduced, defined as the time spent by a generic fluid element to reach position x after entering the reactor [12]. This quantity can be evaluated through the following differential equation:

$$\frac{d\theta}{dx} = \frac{\rho(x)\mathscr{A}(x)}{F(x)} \tag{31}$$

To summarise, the LIR model is made of $(3NC+6)$ equations (namely, Equations (16), (17), (18), (21), (25), (31), (27), (28) and (29)) with $(5NC+12)$ unknowns: $\underline{\omega}(x)$, $\underline{\omega}_0$, $F(x)$, F_0, $\underline{f}(x)$, $f(x)$, $T(x)$, T_0, $T_f(x)$, $\dot{q}(x)$, $\theta(x)$, $\rho(x)$, $c_p(x)$, $\underline{\overline{H}}(x)$, $\underline{\overline{H}}^f(x)$, $\mathscr{A}$, and the reactor length L. Therefore, $(2NC+6)$ degrees of freedom need to be saturated in order to make the problem well-defined.

2.3. Proposed semi-batch to continuous transformation procedure

In order to establish a duality between SBR and tubular reactor in terms of conversion and selectivity, equal mass fractions and temperatures are enforced at any time $t = \theta(x)$:

$$\omega_i(x) = \omega_i^*(\theta(x)) \qquad \forall x \in [0, L] \tag{32}$$

$$T(x) = T^*(\theta(x)) \qquad \forall x \in [0, L] \tag{33}$$

Consequently, the same relation holds true for density and specific heat capacity, i.e., $\rho(x) = \rho^*(\theta(x))$ and $c_p(x) = c_p^*(\theta(x))$. Moreover, the following equality ensures the same reaction time in both reactors:

$$\theta(L) = t_{rxn} \tag{34}$$

where t_{rxn} is the reaction time in the SBR.

Equations (32), (33) and (34) represent $2NC+3$ additional constraints, being the formers valid not only along the reactor but also at the inlet where the BCs (19) and (26) apply (i.e., $\omega_i(0) = \omega_i^*(0) = m_{i,0}^*/m_0^*$ and $T(0) = T_0 = T^*(0) = T_0^*$). Therefore, 3 degrees of freedom remain, which can be saturated by setting arbitrary values of F_0, $\mathscr{A}(x)$ and $T_f(x)$. The most straightforward choice for the latter is:

$$T_f(x) = T_{F^*}(\theta(x)) \tag{35}$$

thus retaining consistency with Equation (33).

Exploiting the same approach reported in detail elsewhere [12], it can be easily shown that the isothermal solution developed to compute the feed policy in the tubular reactor applies also in the non-isothermal case, that is:

$$f_i(x) = \rho(x)\mathscr{A}(x)\frac{F_i^*(\theta(x))}{m^*(\theta(x))} \tag{36}$$

or

$$\frac{f_i}{\mathscr{A}} = \frac{F_i^*(\theta(x))}{V^*(\theta(x))} \tag{37}$$

where $V^* = m^*/\rho^*$ is the reaction volume in the SBR at time $t = \theta(x)$. Consequently:

$$\underline{\omega}^f(x) = \frac{\underline{f}(x)}{f(x)} = \frac{\underline{F}^*(\theta(x))}{F^*(\theta(x))} = \underline{\omega}^{F^*}(\theta(x)) \tag{38}$$

and therefore $\overline{\underline{H}}^f(x) = \overline{\underline{H}}^{F^*}(\theta(x))$ when Equation (35) is applied.

Equation (25) can be recast using Equations (31), (32) and (33) (note that the explicit dependencies on the axial coordinate and elapsed time are dropped in the following to make the equations more readable):

$$Fc_p^* \left.\frac{dT^*}{dt}\right|_{t=\theta} \frac{d\theta}{dx} = \sum_{i=1}^{NC} \frac{f_i}{MW_i}(\overline{H}_i^f - \overline{H}_i^*) - \mathscr{A}\sum_{j=1}^{NR} \Delta H_{R,j}(T^*) r_j(\underline{\omega}^*, T^*) + \dot{q} \tag{39}$$

By introducing Equations (10) and (36) one obtains:

$$\dot{q} = \sum_{i=1}^{NC} \frac{\rho \mathscr{A} F_i^*}{m^* MW_i} (\overline{H}_i^{F^*} - \overline{H}_i^f) + \rho \mathscr{A} \frac{\dot{Q}^*}{m^*} \tag{40}$$

Similarly to Equation (36), this equation is independent on kinetics, provided that the change in time of the physical properties (either evaluated by suitable modelling of the SBR process or by direct measurement of the variables in the real SBR) is known. Therefore, the following derivations are kinetics-free, i.e., the knowledge of the reaction kinetics is not a requirement.

Using Equation (35), the last previous expression reduces to:

$$\dot{q}(x) = \rho(x) \mathscr{A}(x) \frac{\dot{Q}^*(\theta(x))}{m^*(\theta(x))} \tag{41}$$

which has the same functional form of Equation (36), thus implying that the heat flux per unit volume is preserved when the process is transformed from SBR to LIR:

$$\frac{\dot{q}}{\mathscr{A}} = \frac{\dot{Q}^*(\theta(x))}{V^*(\theta(x))} \tag{42}$$

This last equation can be simplified and made more explicit according to the original SBR process heat transfer method (adiabatic, isoperibolic, or diabatic reactor), as discussed in the following. Note that Equations (36) and (41) provide a unique solution for the transformation of a SBR into a LIR. This holds true because of the uniqueness of the relationship $\theta(x)$, provided by the applicability of the Cauchy theorem in Equation (31). Accordingly, the LIR corresponding to a given SBR has a unique design.

It should be noted that cross sectional area and inlet axial flowrate are still degrees of freedom, so the productivity of the equivalent tubular reactor can be arbitrarily chosen. For each component k, the massive productivity of the SBR, $\mathscr{P}_k^*$, and of the LIR, $\mathscr{P}_k$, can be defined as:

$$\mathscr{P}_k^* = \frac{m^*(t_{rxn}) \omega_k^*(t_{rxn})}{t_{proc}} \tag{43}$$

$$\mathscr{P}_k = F(\theta(L)) \omega_k(L) \tag{44}$$

where t_{proc} is the overall process time required for the discontinuous process (accounting for reaction,

cleaning, charging, and so on). The proposed procedure allows to compute the productivity ratio, $R_{\mathscr{P}}$, as:

$$R_{\mathscr{P}} \stackrel{\text{def}}{=} \frac{\mathscr{P}_k}{\mathscr{P}_k^*} = \frac{F_0 t_{proc}}{m_0^*} \tag{45}$$

independently on the selected species k. The last equation is readily worked out by considering that $\theta(L) = t_{rxn}$ and that [12]:

$$\frac{F(\theta(L))}{m^*(t_{rxn})} = \frac{F_0 \left(1 + \int_0^{\theta(L)} \frac{F^*(t)}{m_0^*} dt\right)}{m_0^* + \int_0^{t_{rxn}} F^*(t) dt} = \frac{F_0}{m_0^*} \tag{46}$$

Furthermore, the hold-up (or volume) of the LIR can be defined as:

$$V \stackrel{\text{def}}{=} \int_0^L \mathscr{A}(x) dx \tag{47}$$

and the volume ratio, R_V, between LIR and SBR can be expressed as [12]:

$$R_V \stackrel{\text{def}}{=} \frac{V}{V^*(t_{rxn})} = \frac{\int_0^{t_{rxn}} \frac{F(\theta(x)=t)}{\rho^*(t)} dt}{\frac{m^*(t_{rxn})}{\rho^*(t_{rxn})}} = R_{\mathscr{P}} \frac{\rho^*(t_{rxn})}{F(\theta(L)) t_{rxn}} \left(\frac{t_{rxn}}{t_{proc}}\right) \int_0^{t_{rxn}} \frac{F(t)}{\rho^*(t)} dt \tag{48}$$

According to the density profile in time, it is possible to draw considerations on the relation between productivity and volume ratios. If the density is constant or monotonously decreasing in time, the integral average of the quantity F/ρ^* in the last equation is smaller than its final value $F(\theta(L))/\rho^*(t_{rxn})$, being the flowrate F a strictly increasing function (as evident from Equation (18)). Consequently, being $t_{rxn}/t_{proc} \leq 1$, it will be

$$R_V < R_{\mathscr{P}} \tag{49}$$

meaning that the hold-up is *always decreased by the transformation* when the productivity is kept unchanged or, equivalently, that the productivity is increased when the hold-up is kept constant. Therefore, an effective process intensification can be achieved in both cases. Note that the volume ratio can be smaller than the productivity ratio also for increasing or non-monotonously-decreasing density profiles: even though this is not fully general, we can definitely state that Equation (49) applies in most cases.

For the particular case of constant density, after the integration of Equation (48) one obtains:

$$R_V = R_{\mathscr{P}} \frac{t_{rxn}}{t_{proc}} \left(1 - \frac{\int_0^{t_{rxn}} tF^*(t)dt}{m^*(t_{rxn})t_{rxn}} \right) \tag{50}$$

given that [12]

$$F(\theta) = F_0 \left(1 + \int_0^{\theta} \frac{F^*(t)}{m_0^*} dt \right) \tag{51}$$

The procedure proposed to shift from a SBR-based process into LIR-based one can be summarised as follows:

1. compute $f_i(x)$, $\theta(x)$, and L as discussed in detail for the isothermal case in [12], using the known values of $\rho^*(t)$, $F_i^*(t)$, $\mathscr{A}(x/L)$, and F_0;
2. find $\dot{q}(x)$ using the value of $\dot{Q}^*(t)$ computed using
   a. Equation (40) if SBR and LIR feed temperatures are different;
   b. Equation (41) if SBR and LIR feed temperatures are equal according to Equation (35);

The following paragraphs discuss simpler equations arising from particular cases as well as how to apply the proposed procedure when $\dot{Q}^*(t)$ cannot be measured in the SBR.

2.3.1. Adiabatic SBR process

It can be noted from Equation (41) that an adiabatic SBR is always transformed into an adiabatic LIR, as expected. This is true if the feed temperatures are equal in the SBR and tubular reactor as required by Equation (35). Otherwise, an adiabatic SBR is not transformed into an adiabatic Zwietering-like reactor since the heat exchange should compensate some sensible heat arising from the feed temperature difference.

2.3.2. Diabatic SBR process

With reference to jacketed reactors, an energy balance can be written also for the thermal medium (cooling/heating fluid). Assuming uniform conditions, constant properties, and single phase for the SBR thermal medium, the energy balance equation around the jacket becomes:

$$\begin{cases} m_{tm}^* c_{p,tm}^* \dfrac{dT_{tm}^*}{dt} = F_{tm}^* c_{p,tm}^* (T_{tm,IN}^* - T_{tm}^*) - \dot{Q}^* \\ T_{tm}^*(0) = T_{tm,IN}^*(0) \end{cases} \tag{52}$$

where T_{tm}^* is the thermal medium temperature, m_{tm}^* the jacket hold-up, $c_{p,tm}^*$ the (constant) medium massive specific heat capacity, F_{tm}^* the medium flowrate in the SBR jacket and $T_{tm,IN}^*$ the inlet medium temperature.

The specific heat flow rate of the tubular reactor, $\dot{q}$, can be related to the temperature difference between reactor and jacket through the well established expression:

$$\dot{q}(x) = \mathscr{U}(x)\Pi_e(x)(T_{tm}(x) - T(x)) = \mathscr{U}(x)\Pi_e(x)(T_{tm}(x) - T^*(\theta)) \tag{53}$$

where $\mathscr{U}$ is the LIR (local) global heat exchange coefficient, Π_e the LIR local perimeter of the heat exchange area, and T_{tm} the cooling/heating medium temperature in the LIR jacket. Also the heat flow through the jacket surface of the SBR, $\dot{Q}^*$, can be expressed through a similar expression:

$$\dot{Q}^*(t) = \mathscr{U}^*(t)S^*(t)(T^*_{tm}(t) - T^*(t)) \tag{54}$$

where $\mathscr{U}^*$ is the global heat exchange coefficient and S^* the heat exchange surface in the SBR. Plugging Equations (53) and (54) into Equation (41), one obtains:

$$T_{tm}(x) = T^*(\theta) + \frac{\mathscr{A}(x)}{\mathscr{U}(x)\Pi_e(x)} \frac{\mathscr{U}^*(\theta)S^*(\theta)}{V^*(\theta)} (T^*_{tm}(\theta) - T^*(\theta)) \tag{55}$$

By defining:

$$\epsilon_R(x) \stackrel{\text{def}}{=} \frac{\dfrac{\mathscr{U}(x)\Pi_e(x)}{\mathscr{A}(x)}}{\dfrac{\mathscr{U}^*(\theta)S^*(\theta)}{V^*(\theta)}} \tag{56}$$

the previous expression for $T_{tm}(x)$ can be recast in the general form:

$$T_{tm}(x) = T^*(\theta) + \frac{1}{\epsilon_R(x)} (T^*_{tm}(\theta) - T^*(\theta)) \tag{57}$$

The dimensionless number ϵ_R represents the ratio of heat exchange efficiency between LIR and SBR. Introducing this dimensionless quantity, important conclusions on the transformation procedure can be drawn. $\epsilon_R > 1$ means that the SBR is less efficient in heat removal (or supply) and the coolant temperature will be higher in LIR than in the equivalent SBR (or, reversely, the heating temperature will be lower).
The order of magnitude of $\Pi_e/\mathscr{A}$ can be estimated as $4/D_h$, where D_h is the LIR hydraulic diameter, while the one of S^*/V^* as $4/D^*$, where D^* is the SBR diameter. Consequently, ϵ_R will be a number larger than unity in most cases, being the SBR diameter typically larger than that of the LIR (note that this is true when the heat exchange coefficients of the two reactors do not differ too much).

Plugging Equations (52) and (53) into Equation (41) allows determining another equivalent formulation

for the thermal medium temperature and the thermal efficiency ratio:

$$T_{tm}(x) = T^*(\theta) + \frac{F^*_{tm} c^*_{p,tm} \rho \mathscr{A}}{\mathscr{U}(x)\Pi_e(x) m^*(\theta)} \left(T^*_{tm,IN}(\theta) - T^*_{tm}(\theta) - \frac{m^*_{tm}}{F^*_{tm}} \left. \frac{dT^*_{tm}}{dt} \right|_{t=\theta} \right) \tag{58}$$

$$\epsilon_R(x) = \frac{\mathscr{U}(x)\Pi_e(x) m^*(\theta)}{F^*_{tm} c^*_{p,tm} \rho \mathscr{A}} \frac{T^*_{tm}(\theta) - T^*(\theta)}{T^*_{tm,IN}(\theta) - T^*_{tm}(\theta) - \frac{m^*_{tm}}{F^*_{tm}} \left. \frac{dT^*_{tm}}{dt} \right|_{t=\theta}} \tag{59}$$

With respect to Equation (56), Equation (59) represents an alternative expression for ϵ_R, which can become more convenient according to the available data.

By defining the following dimensionless groups, where T^* is taken as a reference temperature,

$$\tau^*(t) \stackrel{\text{def}}{=} \frac{T^*_{tm}(t)}{T^*(t)} \tag{60}$$

$$\tau(x) \stackrel{\text{def}}{=} \frac{T_{tm}(x)}{T^*(\theta(x))} \tag{61}$$

Equation (57) can be recast as

$$\tau(x) = \tau^*(\theta(x)) \frac{1}{\epsilon_R(x)} + \left(1 - \frac{1}{\epsilon_R(x)} \right) \tag{62}$$

which becomes a linear relationship between the two dimensionless quantities when ϵ_R is constant.

Together with Equation (36), this last relationship can replace Equation (41) to constitute a more convenient design procedure for transforming a SBR into a LIR in terms of thermal medium temperature profile along the axial coordinate. For example, Equation (62) can be used to draw the diagram τ vs. τ^* reported in Figure 3, where the different regions of the plot indicate whether the continuous tubular reactor is more efficient than the original SBR in terms of heat exchange. This "master plot" is divided in four main quadrants, according to whether the reactor is cooled or heated via the thermal medium. When $\tau^* < 1$, cooling is performed and the transformation can lead to a cooled LIR only, independently on the efficiency ratio. This implies that the region $(\tau^* < 1, \tau > 1)$ is unfeasible for the transformation. Similarly, a heated SBR can be transformed into a heated LIR only, meaning the region $(\tau^* > 1, \tau < 1)$ is inaccessible to the transformation. A generic process transformation will then be represented by a parametric curve on the master plot, always crossing the point $\tau = \tau^* = 1$, where the curve parameter is space (the axial coordinate, x) or time (the elapsed time, θ). The point $\tau = \tau^* = 1$ belongs to the curve if process temperature and cooling/heating temperature cross one to each other or if the SBR is cooled/heated before starting and/or

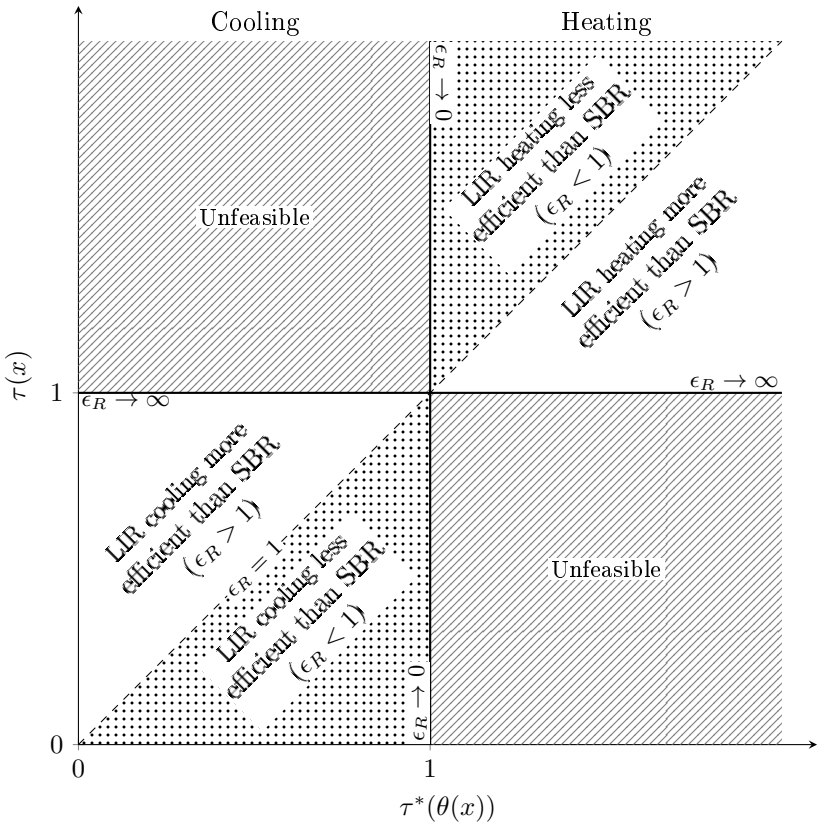

Figure 3: Master plot for the comparison of tubular reactor cooling/heating efficiency with respect to SBR.

after ending the reaction. In typical cases, the curve $\tau(\tau^*)$ is expected to fall in the white regions of the graph, where heat transfer is more efficient in the LIR than in the SBR, i.e., $\epsilon_R > 1$.

2.3.3. Isoperibolic SBR process

Since $T^*_{tm} = T^*_{tm,IN} = \text{const}$ in this case, the energy balance for the thermal medium is no longer required and $\dot{Q}^*$ can be computed using Equation (54). Consequently, Equation (59) can be used to compute ϵ_R and the thermal medium temperature profile in the LIR becomes:

$$T_{tm}(x) = T^*(\theta) + \frac{1}{\epsilon_R(x)}(T^*_{tm,IN} - T^*(\theta)) \tag{63}$$

Note that an isoperibolic SBR is not necessarily transformed into an isoperibolic tubular reactor. This happens only in the case $\epsilon_R(x) = 1$ for the entire reactor length, which is represented in Figure 3 by the diagonal $\tau = \tau^*$.

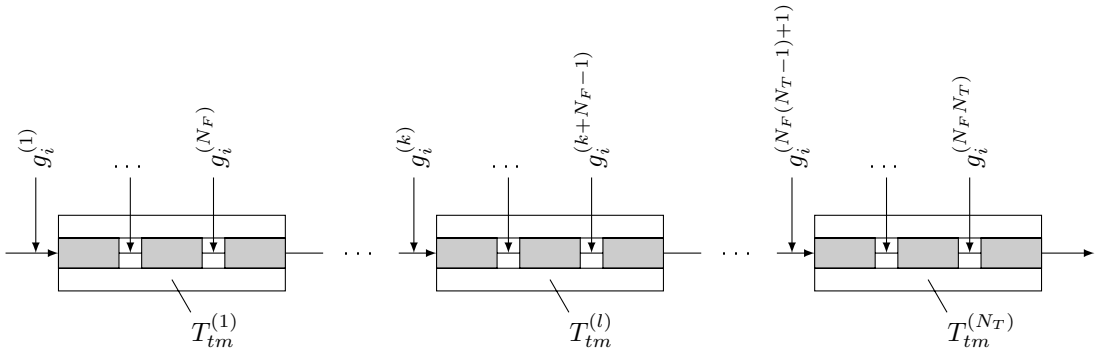

Figure 4: Approximation of the continuous lateral feed injections, $f_i(x)$, and thermal medium temperature, $T_{tm}(x)$, with N_T isoperibolic jackets of temperature $T_{tm}^{(l)}$ and N_F discrete side injections, $g_i^{(k)}$, distributed along each discrete jacket.

2.3.4. Batch reactor process

The batch reactor (BR) is a particular case of the SBR transformation procedure, where $F^*(t) = 0$. Therefore, no lateral feed is required in the tubular reactor and ϵ_R depends only on physical properties and cross sectional area of the tubular reactor. If the former remain constant during the reaction and constant cross sectional area is assumed, ϵ_R is also constant and the corresponding representation in Figure 3 is a straight line with slope equal to $1/\epsilon_R$.

2.4. The master plot

The master plot represented in Figure 3 can be conveniently used to visualise differences between the temperatures of the thermal media in the two reactors, SBR and equivalent LIR. However, the same representation can be helpful in other cases, for example to assess the thermal equivalence between the "rigorous" LIR and alternative continuous configurations. In fact, it is extremely difficult to establish a defined axial profile for the temperature of the thermal fluid and a discretisation approach (as the one previously explored in the isothermal case with respect to the axial profile of the lateral feed, [12]) can be considered also in this case. The corresponding reactor will be indicated as discretised LIR, d-LIR. Again, the assumption of plug flow is applied also to the d-LIR, in analogy with the LIR. This implies that the discrete injections must be implemented such that complete radial mixing is achieved almost instantaneously.

The effect of the discretisation of the feed was already investigated for the isothermal case [12], showing that a sufficiently large number of discrete injections allows a d-LIR to well reproduce the behaviour of the LIR. In a similar way, also the jacket can be discretised through a series of independent jackets, each one working under isoperibolic conditions as sketched in Figure 4. Namely N_T isoperibolic jackets are

Table 1: Data for the generic reaction example.

t_{rxn}	[s]	1000
$m_0^* = m_{A,0}^*$	[kg]	1000
T_{tm}^*	[K]	298.15
ρ	[kg m^{-3}]	900
μ	[cP]	1
c_p	[J kg^{-1} K^{-1}]	2000
Pr	[-]	3.3
$\mathscr{U}^*$	[W m^{-2} K^{-1}]	7000

considered, each one having N_F feed injections. It should be noted that, from a practical point of view, it is easier to discretise the lateral feed policy (e.g., with injectors), rather than the thermal medium temperature profile (which requires a particular manufacturing). Similarly to the isoperibolic LIR, the transformation of an isoperibolic SBR process into an isoperibolic d-LIR with discrete jackets can be represented on the master plot as a set of straight lines (segments) parallel to the diagonal. Therefore, a fitting procedure of this piecewise linear function can be performed to design a d-LIR, starting from the LIR curve on the phase diagram. This fitting procedure is quite arbitrary and the number of discrete jackets as well as each specific length can be chosen according to any criterion (practical or theoretical constraints). Given a jacket configuration, the different jacket temperatures can be found by fitting. The use of a finite number of jackets results in discrepancies between the original LIR and the specific d-LIR; of course, such difference is expected to vanish when N_T approaches infinity.

As an example, let us consider a generic (unknown) reaction of two species, A and B, carried out in a SBR with the following feed policy:

$$F_A^*(t) = 0, \qquad F_B^*(t) = 1\,\mathrm{kg\,s^{-1}} \tag{64}$$

Moreover, let us assume that the measured reactor temperature profile of the hypothetical process can be approximated by:

$$T^*[\mathrm{K}](t[\mathrm{s}]) = 298.15 + 10e^{-0.003t}(1 - e^{-0.01t}) \tag{65}$$

and that the heat exchange surface changes in time according to a linear law:

$$S^*[\mathrm{m}^2](t[\mathrm{s}]) = 3 + 5 \times 10^{-4}t \tag{66}$$

All other parameters of the hypothetical process are given in Table 1.

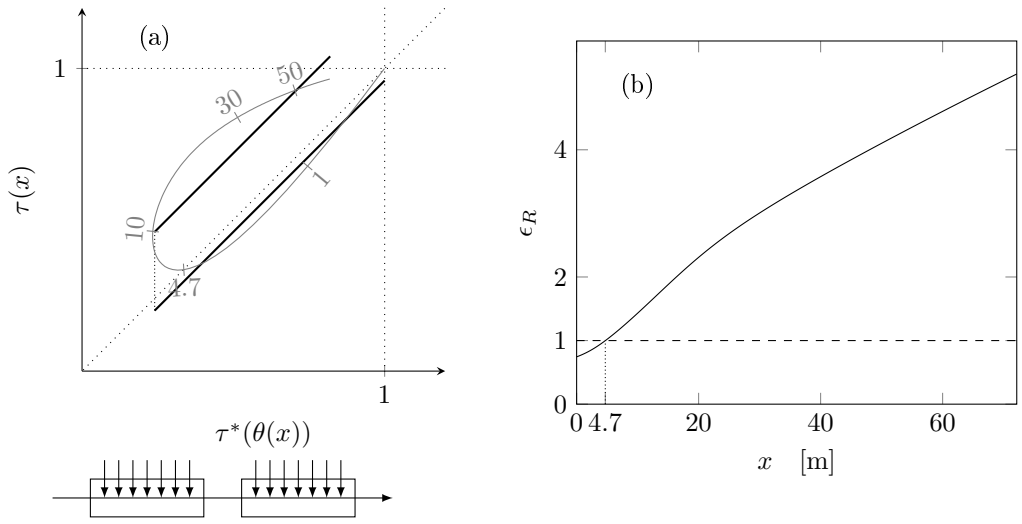

Figure 5: Example transformation: (a) master plot for LIR, labelled with axial coordinate [m], and a possible d-LIR using two different jackets; (b) LIR heat exchange efficiency ratio as a function of the axial coordinate.

A pipe of diameter 5 cm is available for the transformation procedure. According to the inlet flowrate, different profiles will be obtained in the master plot as the local heat exchange coefficient in the LIR depends on the fluid velocity according to well known relations [14].

Figure 5a is the master plot of a LIR where the inlet flowrate was set to $0.085\,\mathrm{kg\,s^{-1}}$ (thin curve) and a possible discretisation (thick straight lines) using two different isoperibolic jacket portions ($N_T = 2$) working at two different temperatures. The LIR curve is labelled by the values of the corresponding axial coordinate. Note that the initial and final points of LIR curve and d-LIR lines are not coincident. Figure 5b reports the values of ϵ_R as function of the axial coordinate and it can be seen that most of the LIR is more efficient in heat exchange than the SBR ($\epsilon_R > 1$). In order to trace the d-LIR curve, only the value of N_T is required, while the one of N_F is not necessary (and was arbitrarily set equal to 7 in the figure for illustrative purposes only). Notably, the whole procedure is kinetics-free, as only some measured values (such as T^* and S^*) were needed to transform the discontinuous process into a continuous one, without knowing the reaction mechanism.

3. Case study

To illustrate potentials and limits of the proposed procedure, a case study involving a copolymerisation process was investigated. Note that the knowledge of the chemical kinetics is exploited in the following only to develop the optimal reaction path in the SBR. If such a recipe is already known (for instance,

from laboratory tests or even from the industrial plant experience), no kinetic information are required, as already mentioned. This is evident from the two Equations (36) and (62) which constitute the proposed set of equations aimed to evaluate the side feed policy and the cooling temperature profile along the axial coordinate of the equivalent tubular reactor.

3.1. SBR feed policy design

As discussed in detail elsewhere [12], the optimal feed policy to obtain constant product composition in a free-radical copolymerisation process carried out in solution using a SBR can be computed through the power feed technique [10, 11]. Monomer A (the most reactive) is continuously fed to the reactor, while monomer B is initially fully charged into the vessel. Molar balance equations can be written in terms of number of moles of the two species, n_A and n_B, and for the total mass, m^*, as follows:

$$\begin{cases} \dfrac{dn_A}{dt} = \dot{N}_A(t) - R_A V^* \\ \dfrac{dn_B}{dt} = -R_B V^* \\ \dfrac{dm^*}{dt} = \dot{N}_A(t) MW_A \end{cases} \tag{67}$$

where $\dot{N}_A$ is the unknown feed policy of A, R_i $(= k^*_{pi} c_{R\bullet} c_i)$ the species i molar production rate, c_i the species i molar concentration, $c_{R\bullet}$ the total concentration of radicals $(= \sqrt{R_I / k^*_t})$, and MW_i the molecular weight of species i. Using the long chain approximation (LCA) [15] and the pseudo-kinetic approach [16], k^*_{pi} can be computed from the monomeric composition as summarised in Table 2. All kinetic constants are assumed to depend on temperature according to the Arrhenius law:

$$k = k^0 \exp\left(-\frac{E_a}{RT}\right) \tag{68}$$

where k^0 is the pre-exponential factor, E_a the activation energy, and R the ideal gas constant.

Since temperature can change during time, the Mayo-Lewis plot [17] of the considered system varies in time as well, even if it is well-known that this variation is frequently minor. Accordingly, in order to produce a copolymer with prescribed molar monomeric ratio, ϕ_A, the monomeric fraction, X_A, in the reacting mass must be properly controlled, accounting also for the temperature change. Note that, while in the isothermal case constant monomer fraction or constant polymer monomeric ratio can be used interchangeably, this is not true in the non-isothermal case.

Table 2: Definitions for the non-isothermal copolymerisation case study.

Variable	Definition
R_I	$2\eta k_d c_{I_2} \approx \text{const}$
k^*_{pA}	$k_{pAA}p_A + k_{pBA}p_B$
k^*_{pB}	$k_{pBB}p_B + k_{pAB}p_A$
p_A	$\dfrac{k_{pBA}c_A}{k_{pAB}c_B + k_{pBA}c_A}$
p_B	$\dfrac{k_{pAB}c_B}{k_{pAB}c_B + k_{pBA}c_A}$
k^*_t	$k_{tAA}p_A^2 + 2k_{tAB}p_Ap_B + k_{tBB}p_B^2$

The energy balance equation in this case is:

$$m^* c_p \frac{dT^*}{dt} = \Delta\widetilde{H}_A R_A V^* + \Delta\widetilde{H}_B R_B V^* + \dot{N}_A c_{p,A}(T_{F^*} - T^*) + \mathscr{U}^* S^*(T^*_{tm} - T^*) \tag{69}$$

where c_p is the average massive heat capacity, and $\Delta\widetilde{H}_A$ and $\Delta\widetilde{H}_B$ are the polymerisation heats for monomer A and B, respectively. The heat exchange surface is assumed to vary with the reaction volume in a cylindrical reactor of given diameter $D^* = 1\,\text{m}$ according to:

$$\begin{aligned} S^* &= \frac{\pi D^{*2}}{4} + \frac{4}{D^*}V^* \\ &= 0.7854 + 4V^* = 0.7854 + 4\frac{m^*}{\rho} \end{aligned} \tag{70}$$

while, for the sake of simplicity, it is assumed that the global heat exchange coefficient and the thermal medium (coolant) temperature remain constant throughout the (isoperibolic) process, as well as all physical and chemical properties.

In order to guarantee a polymer with constant composition, the following algebraic constraint has to be fulfilled:

$$\phi_A(t) = \phi_A(0) \tag{71}$$

where the instantaneous value of the polymer composition is given by the Mayo-Lewis equation:

$$\begin{aligned} \phi_A &= \frac{(r_A - 1)X_A^2 + X_A}{(r_A - 2)X_A^2 + 2X_A + r_B(1 - X_A)^2} \\ X_A &= \frac{n_A}{n_A + n_B} \end{aligned} \tag{72}$$

Table 3: Data for the non-isothermal copolymerisation.

		A	B
MW_i	$[\mathrm{kg\,kmol^{-1}}]$	50	80
ρ	$[\mathrm{kg\,m^{-3}}]$	900	
μ	[cP]	1	
c_p	$[\mathrm{J\,kg^{-1}\,K^{-1}}]$	2000	
Pr	[-]	3.3	
k^0_{pii}	$[\mathrm{m^3\,kmol^{-1}\,s^{-1}}]$	1.0×10^6	1.5×10^6
$E_{a,pii}/R$	[K]	1400	1800
k^0_{pij}	$[\mathrm{m^3\,kmol^{-1}\,s^{-1}}]$	1.0×10^5	1.0×10^5
$E_{a,pij}/R$	[K]	2000	1200
$\Delta\widetilde{H}_i$	$[\mathrm{kJ\,mol^{-1}}]$	-20	-20
k^0_{tii}	$[\mathrm{m^3\,kmol^{-1}\,s^{-1}}]$	1.0×10^8	1.0×10^8
$E_{a,tii}/R$	[K]	600	600
k^0_{tij}	$[\mathrm{m^3\,kmol^{-1}\,s^{-1}}]$	1.0×10^7	
$E_{a,tij}/R$	[K]	500	
ηk_d	$[\mathrm{s^{-1}}]$	5×10^{-4}	
$\mathscr{U}^*$	$\mathrm{W\,m^{-2}\,K^{-1}}$	3000	

where $r_i = k_{pii}/k_{pij}$ is the reactivity ratio of species i.

Initial values for molar, mass and energy balances are $n_{i,0}$, $m_0 = n_{A,0}MW_A + n_{B,0}MW_B$, and T_0^*, respectively. Species initial quantities are once more obtained from the Mayo-Lewis plot, given the desired copolymer productivity and monomer ratio. The aforementioned Equations (67), (69) and (71) constitute a DAE system, which can be solved numerically to find, among the others, the unknown feed policy $\dot{N}_A(t)$. The system integration stops when the fed quantity of A corresponds to the one necessary to achieve the desired polymer amount.

The values of all model parameters are summarised in Table 3. Assuming a required production of 1 t of copolymer made of 70 wt% of A (corresponding to $\phi_A = 0.79$), one obtains $n_{A,0} = 1.26\,\mathrm{kmol}$, $n_{B,0} = 3.75\,\mathrm{kmol}$, and $m_0^* = 363\,\mathrm{kg}$. An initiator concentration of 0.5 mol% is used, while initial temperature, coolant and inlet temperatures are assumed to be the same and equal to 25 °C. Setting a process time of 1000 s, the overall fed quantity is 1.20 kmol (the Mayo-Lewis plot would have imposed 1.27 kmol, requiring a much longer time, as discussed elsewhere [12]). The power feed policy is shown in Figure 6 along with the monomer fraction, reactor temperature and cooling temperature profiles in time. Notably, the feed policy is no more a decreasing exponential function of time (as it was in the isothermal case [12]). Furthermore, even though the copolymer composition is constant, the monomer mixture composition is changing in time due to the temperature variation.

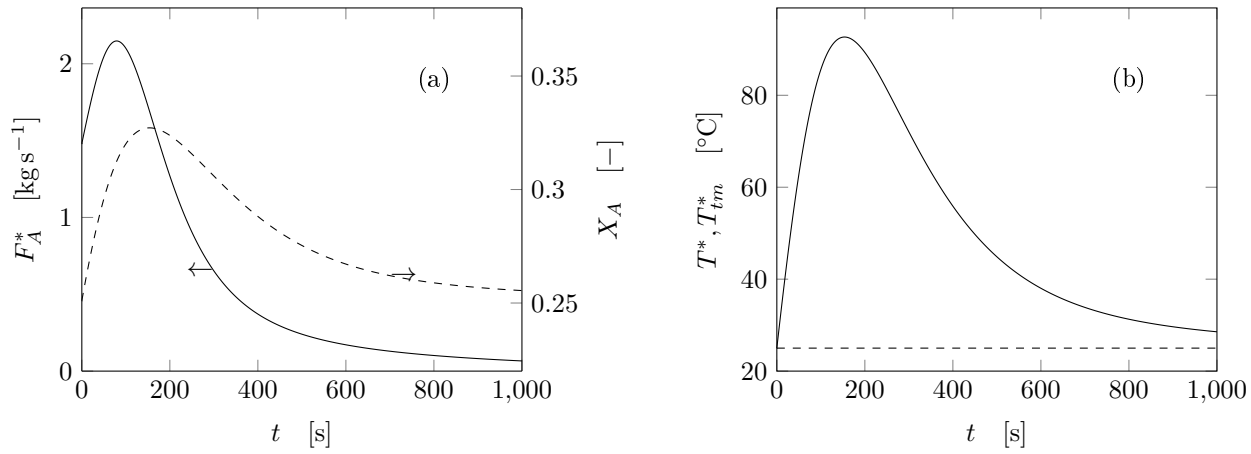

Figure 6: (a) SBR monomer feed policy, F_A (solid curve), and monomeric fraction, X_A (dashed curve), in time according to the power feed procedure; (b) SBR temperature, T^* (solid curve), and coolant temperature, T_{tm}^* (dashed curve).

3.2. Transition to a continuous tubular reactor

The aforementioned procedure for the transformation of the copolymerisation reactor is adopted assuming that the feed temperature is uniform along the axial coordinate and equal to the SBR feed temperature (i.e., 25 °C). The Churchill equation [14] was used to estimate the global heat transfer coefficient, considering internal convection as the heat transfer limiting phenomenon. Reactor diameter of 8 cm is assumed for design. The inlet flowrate can be set to guarantee the same productivity of the SBR ($t_{proc} = 1.3t_{rxn}$ is assumed). This would lead anyway to a very long (140 m) reactor, becoming impractical. Therefore, the inlet flowrate is reduced to shorten the LIR while the productivity is matched by using several reactors in parallel. For example, selecting two reactors, each having half the productivity of the original SBR, one obtains about-half-long reactors, each one with inlet flowrate equal to 0.14 kg s^{-1}, according to Equation (45).

Feed policy and coolant temperature along the axial coordinate computed through Equations (36) and (62) are reported in Figure 7. Solving the mass and energy balance equations for the LIR together with these feed and cooling temperature profiles leads to perfectly overlapping temperature and composition profiles of LIR and SBR, thus producing constant composition copolymer throughout the entire reactor at $\phi_A = 0.79$. As already mentioned, the isoperibolic SBR is transformed into a non-isoperibolic tubular reactor. The final configuration will then be made of two tubular reactors in parallel, each one 70.8 m long and with volume of 0.36 m^3. Therefore, the total reaction volume is 0.72 m^3, corresponding to $R_V = 0.72$

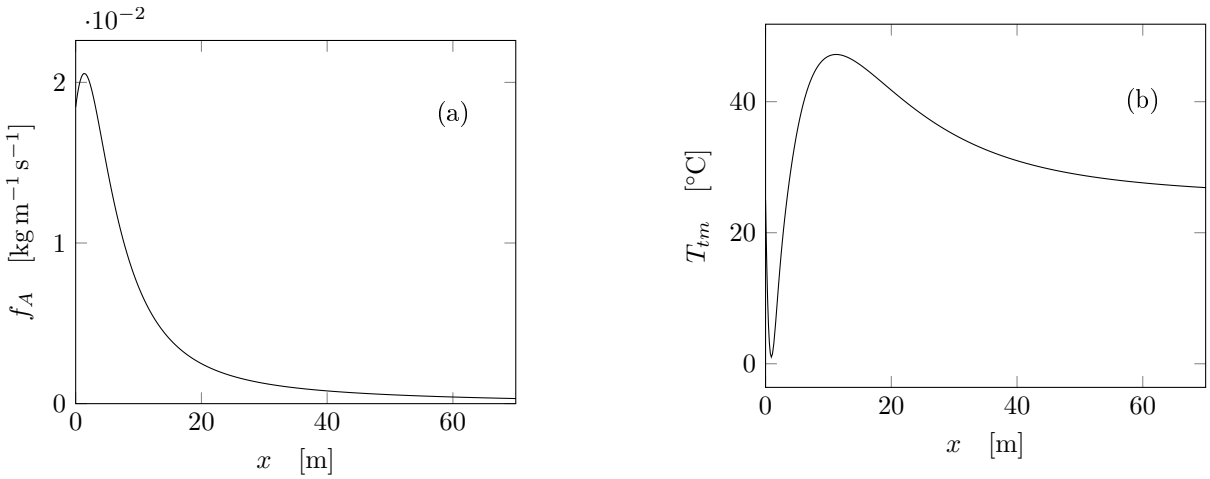

Figure 7: (a) LIR monomer lateral feed policy and (b) thermal medium temperature along the axial coordinate.

(SBR volume was close to 1 m^3). A reduction of the hold-up by almost 30 % is achieved even when using two LIRs in parallel, with an appreciable process intensification: the LIR configuration allows increasing the volume specific productivity by about 40 % with respect to the SBR one. The corresponding master plot is shown in Figure 8. Notably, the transition from SBR to LIR results in a tubular reactor which is initially less efficient than the SBR in terms of cooling (the LIR coolant temperature is below that of the SBR along the first 4.7 m). As the velocity in the tubular reactor increases due to the lateral injections, the LIR cooling efficiency increases and the coolant temperature of the tubular reactor becomes higher than that of the SBR.

To better assess the power of the developed transformation approach, an isoperibolic LIR was also simulated assuming the same coolant temperature as in the SBR (an approach which could be thought as an attractive short-cut to implement the transition to a continuous reactor). In this case, composition and temperature profiles significantly differ from those of the original SBR, leading to a cumulative composition of the outlet copolymer that differs of about 6 % with respect to the desired value. Furthermore, along the axial coordinate, local (instantaneous) deviations as large as about 15 % in the monomeric ratio were found. This heterogeneity can be detrimental for the copolymer quality, thus proving the superior performance of the proposed approach.

Finally, let us explore the performance of a more practical version of the designed LIR, that is the use of N_T isoperibolic jackets in series (the previously defined d-LIR) also discretising the feed flowrates into N_F equally spaced injections per single reactor portion. As shown in Figure 4, this approach results in a

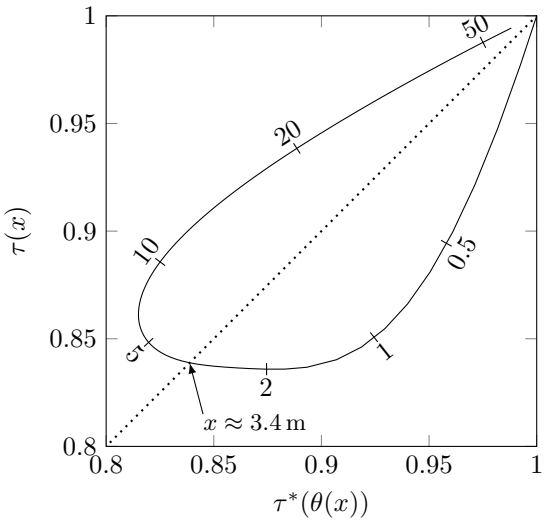

Figure 8: Master plot for the copolymerisation case study reporting LIR vs. SBR dimensionless temperatures. Some values of the axial coordinate of the tubular reactor are also reported on the curve.

total number of feed injections equal to $N_T N_F$. In order to estimate the performance of the d-LIR, mass and energy balance equations were solved for each portion of the tubular reactor without side injections. The generic i-th portion has a length of $\delta L = L/(N_T N_F)$ and is fed with a flowrate equal to the sum of the flowrates leaving the previous section and the one which should be fed laterally (see Figure 4). The latter is given by:

$$g_A^{(k)} = \int_{(k-1)\delta L}^{k\delta L} f_A(x)dx \tag{73}$$

where $k = 1, \ldots, N_T N_F$. Every jacket has a length of $N_F \delta L$ and the coolant temperature of each jacket can be arbitrarily chosen. Even though multiple choices of the coolant temperature are possible, a reasonable value could be the integral average of the predicted coolant temperature profile of the LIR:

$$T_{tm}^{(l)} = \frac{1}{N_F \delta L} \int_{(l-1)N_F\delta L}^{lN_F\delta L} T_{tm}(x)dx \tag{74}$$

where $l = 1, \ldots, N_T$. Whatever are the selected $T_{tm}^{(l)}$ values, the impact of the discretisation on the reactor performance can be expressed as percentage deviation from the desired molar monomeric ratio, $\Delta\phi$, which can be computed as:

$$\Delta\phi = \frac{1}{L} \int_0^L \left| \frac{(R_A + R_B)\phi_A - (R_A^d + R_B^d)\phi_A^d}{(R_A + R_B)\phi_A(L)} \right| dx \cdot 100 \tag{75}$$

where ϕ_A is the (constant) desired value of the monomer ratio, ϕ_A^d the actual profile of the same quantity

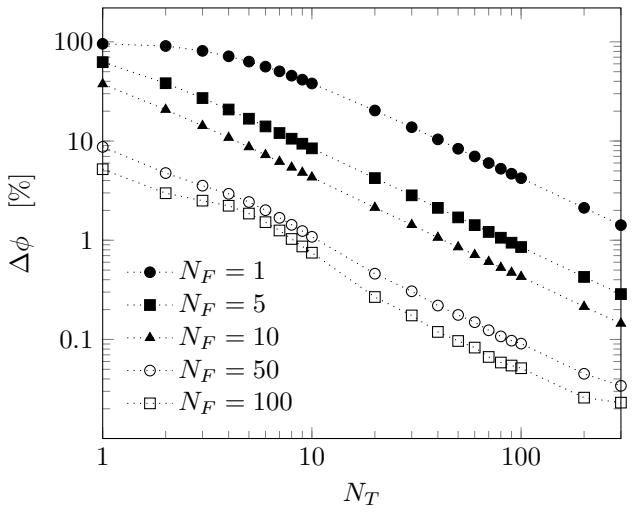

Figure 9: Percent difference of the outlet copolymer monomeric ratio with respect to the rigorous transformation as a function of the discretisation parameters N_T and N_F.

in the d-LIR, and R_i and R_i^d are the production/consumption rate of species i in the LIR and d-LIR, respectively. This quality parameter accounts for the entire profile of the monomer ratio in the discretised reactor and weights it according to the sum of both monomer consumption rates, which is equivalent (except for the sign) to the production rate of the polymer. Consequently, $\Delta\phi$ is a representation of the quality of all the polymer produced in the reactor in terms of cumulative composition.

The results are reported as parametric curves $\Delta\phi(N_T, N_F)$ with parameter N_F in Figure 9. As expected, the performance difference between the continuous and the discretised reactors decreases at increasing number of discretisations, following an almost linear trend on logarithmic scale (i.e., it follows an exponential decrease). From a practical point of view, it will be preferable to choose a configuration with low N_T so that the number of different jacket temperatures is low. The configuration with three jackets and fifty injections each (which means one injection every 47 cm) is an acceptable compromise to obtain deviations below 3 %.

4. Conclusions

The previously developed procedure for the transformation of an isothermal SBR-based process into a LIR was extended to non-isothermal processes involving single-phase reactions. The lateral feed policy can be computed as in the isothermal case, while a suitable thermal medium temperature profile must be enforced to guarantee equal performance. The continuous tubular reactor, with the rigorously computed profiles, guarantees the same performance as the original SBR. Furthermore, its productivity can be chosen

arbitrarily.

In addition to the information required for the isothermal case (i.e., the density and the feed policy as a function of time in the original SBR process), information on the heat exchange rate in the original SBR are required. These can be given as coolant/heating medium temperatures, heat exchange coefficient and exchange area in time, or directly as heat flux in time. Such information can be derived from a numerical model of the SBR process once all the kinetic parameters involved in the chemical mechanism are known, but they can be obtained by on-line measurements on the industrial SBR process, therefore making the proposed procedure kinetics-free. Moreover, the developed procedure is applicable to any kind of homogeneous reaction without requiring information on the specific chemical mechanism.

Finally, the case study of an industrial copolymerisation demonstrated how the proposed method can be adopted to successfully transform even very complex systems. The rigorously computed feeding policy and coolant temperature profiles were compared to the more trivial solution of an isoperibolic tubular reactor, which was not successful in reproducing the desired monomeric ratio. A parametric analysis on the number of discrete side injections and cooling jackets used to mimic the continuous profiles demonstrated the relevance of approximating correctly both the lateral feed and the thermal medium temperature profiles.

Acknowledgements

Financial support of Innovhub for one of us (FF) is gratefully acknowledged.

Nomenclature

$\mathscr{A}$	LIR cross sectional area [m^2]
c	Molar concentration [$\mathrm{kmol\,m^{-3}}$]
c_p^*	SBR mass-specific heat capacity [$\mathrm{J\,kg^{-1}\,K^{-1}}$]
c_p	LIR mass-specific heat capacity [$\mathrm{J\,kg^{-1}\,K^{-1}}$]
$c_{p,tm}^*$	SBR thermal medium mass-specific heat capacity [$\mathrm{J\,kg^{-1}\,K^{-1}}$]
$c_{p,tm}$	LIR thermal medium mass-specific heat capacity [$\mathrm{J\,kg^{-1}\,K^{-1}}$]
D^*	SBR diameter [m]
D_h	LIR hydraulic diameter [m]
E_a	Activation energy [$\mathrm{J\,mol^{-1}}$]

F^* SBR feedrate [$\mathrm{kg\,s^{-1}}$]

F LIR flowrate [$\mathrm{kg\,s^{-1}}$]

F^*_{tm} SBR thermal medium flowrate [$\mathrm{kg\,s^{-1}}$]

F_{tm} LIR thermal medium flowrate [$\mathrm{kg\,s^{-1}}$]

f LIR distributed feedrate [$\mathrm{kg\,s^{-1}\,m^{-1}}$]

g d-LIR discrete feedrate [$\mathrm{kg\,s^{-1}}$]

H^* SBR enthalpy [J]

$\dot{H}$ LIR enthalpy flow [W]

$\dot{H}^{F^*}$ SBR feed enthalpy flow [W]

$\dot{H}^f$ LIR feed enthalpy flow [W]

k Reaction rate constant

k^0 Reaction rate pre-exponential factor

k_d Dissociation rate constant [$\mathrm{s^{-1}}$]

$\tilde{k}_d$ Decay rate [$\mathrm{s^{-1}}$]

k_p Propagation rate constant [$\mathrm{m^3\,kmol^{-1}\,s^{-1}}$]

k_t Termination rate constant [$\mathrm{m^3\,kmol^{-1}\,s^{-1}}$]

L LIR length [m]

MW Molecular weight [$\mathrm{kg\,kmol^{-1}}$]

m^* SBR mass [kg]

m^*_{tm} SBR jacket hold-up [kg]

$\dot{N}$ SBR molar feedrate [$\mathrm{kmol\,s^{-1}}$]

N_F Number of discrete feeds per jacket [-]

N_T Number of discrete jackets [-]

n SBR molar quantity [kmol]

NC Number of components (species) [-]

Pr Prandtl number [-]

$\dot{Q}^*$ SBR heat flow [W]

$\dot{q}$ LIR specific heat flow [$\mathrm{W\,m^{-1}}$]

R Ideal gas constant, $8.314\,\mathrm{J\,mol^{-1}\,K^{-1}}$

R_i i-th species molar production rate [$\mathrm{kmol\,m^{-3}\,s^{-1}}$]

$R_{\mathscr{P}}$ Productivity ratio [-]

R_V Volume ratio [-]

r Molar reaction rate [$\mathrm{kmol\,m^{-3}\,s^{-1}}$]

r_i i-th species reactivity ratio [-]

S^* SBR heat exchange surface [$\mathrm{m^2}$]

T^* SBR temperature [K]

T LIR temperature [K]

T_{F^*} SBR feed temperature [K]

T_f LIR feed temperature [K]

T^*_{tm} SBR thermal medium temperature [K]

T_{tm} LIR thermal medium temperature [K]

t Time [s]

t_{proc} Overall process time [s]

t_{rxn} Reaction time [s]

$\mathscr{U}^*$ SBR global heat exchange coefficient [$\mathrm{W\,m^{-2}\,K^{-1}}$]

$\mathscr{U}$ LIR (local) global heat exchange coefficient [$\mathrm{W\,m^{-2}\,K^{-1}}$]

V^* SBR volume [$\mathrm{m^3}$]

V LIR hold-up [$\mathrm{m^3}$]

X Monomeric fraction [-]

x Axial coordinate [m]

Greek symbols

ΔH_R Reaction enthalpy [$\mathrm{J\,mol^{-1}}$]

ϵ_R Heat exchange efficiency ratio [-]

η Initiator efficiency [-]

μ Dynamic viscosity [Pa s]

ϕ Monomer molar fraction in copolymer [-]

$\dot{\Omega}_i$ i-th species massive production rate [$\mathrm{kg\,m^{-3}\,s^{-1}}$]

ω^* SBR mass fraction [-]

ω LIR mass fraction [-]

ω^{F^*} SBR feed mass fraction [-]

ω^f LIR feed mass fraction [-]

Π_e LIR perimeter of heat exchange area [m]

ρ^* SBR density [$\mathrm{kg\,m^{-3}}$]

ρ LIR density [$\mathrm{kg\,m^{-3}}$]

τ^* SBR dimensionless temperature [-]

τ LIR dimensionless temperature [-]

θ Elapsed time [s]

Other symbols

0 Initial value (subscript)

IN Inlet value (subscript)

i Relative to species i (subscript)

j Relative to reaction j (subscript)

(k) Discrete feed index (superscript)

(l) Discrete jacket index (superscript)

$\underline{\cdot}$ Vectorial quantity $\cdot$

$\bar{\cdot}$ Partial molar quantity $\cdot$

References

[1] M. Movsisyan, E. I. P. Delbeke, J. K. E. T. Berton, C. Battilocchio, S. V. Ley, C. V. Stevens, Taming hazardous chemistry by continuous flow technology, Chem. Soc. Rev. 45 (2016) 4892–4928.

[2] R. Gérardy, N. Emmanuel, T. Toupy, V.-E. Kassin, N. N. Tshibalonza, M. Schmitz, J.-C. M. Monbaliu, Continuous flow organic chemistry: Successes and pitfalls at the interface with current societal challenges, European Journal of Organic Chemistry 2018 (20-21) (2018) 2301–2351.

[3] Z. Anxionnaz, M. Cabassud, C. Gourdon, P. Tochon, Transposition of an exothermic reaction from a batch reactor to an intensified continuous one, Heat Transfer Engineering 31 (9) (2010) 788–797.

[4] F. Maestri, R. Rota, Kinetic-free safe optimization of a semibatch runaway reaction: the nitration of 4-chloro benzotrifluoride, Industrial & Engineering Chemistry Research 55 (2016) 12786–12794.

[5] S. Ferrouillat, P. Tochon, D. Della Valle, H. Peerhossaini, Open loop thermal control of exothermal chemical reactions in multifunctional heat exchangers, International Journal of Heat and Mass Transfer 49 (2006) 2479–2490.

[6] Z. Anxionnaz, M. Cabassud, C. Gourdon, P. Tochon, Heat exchanger/reactors (hex reactors): Concepts, technologies: State-of-the-art, Chemical Engineering and Processing 47 (2008) 2029–2050.

[7] P. Zhang, N. Weeranoppanant, D. A. Thomas, K. Tahara, T. Stelzer, M. G. Russell, M. O'Mahony, A. S. Myerson, H. Lin, L. P. Kelly, K. F. Jensen, T. F. Jamison, C. Dai, Y. Cui, N. Briggs, R. L. Beingessner, A. Adamo, Advanced continuous flow platform for on-demand pharmaceutical manufacturing.

[8] C. H. Phillips, G. Lauschke, H. Peerhossaini, Intensification of batch chemical processes by using integrated chemical reactor-heat exchangers, Applied Thermal Engineering 17 (8–10) (1997) 809–824.

[9] L. S. Pontryagin, Mathematical theory of optimal processes, CRC press, 1987.

[10] D. R. Bassett, K. L. Hoy, Nonuniform Emulsion Polymers, ACS Publications, 1981, Ch. 23, pp. 371–387.

[11] J. C. De La Cal, A. Echevarria, G. R. Meira, J. M. Asua, Minimum-time strategy to produce nonuniform emulsion copolymers. i. theory, Journal of Applied Polymer Science 57 (9) (1995) 1063–1074.

[12] F. Florit, V. Busini, G. Storti, R. Rota, From semi-batch to continuous tubular reactors: A kinetics-free approach, Chemical Engineering Journal 354 (2018) 1007–1017.

[13] T. N. Zwietering, The degree of mixing in continuous flow systems, Chemical Engineering Science 11 (1) (1959) 1–15.

[14] R. H. Perry, D. W. Green, Perry's Chemical Engineer's Handbook, 2008.

[15] G. R. Gavalas, The long chain approximation in free radical reaction systems, Chemical Engineering Science 21 (2) (1966) 133–142.

[16] H. Tobita, A. E. Hamielec, Kinetics of free-radical copolymerization: the pseudo-kinetic rate constant method, Polymer 32 (14) (1991) 2641–2647.

[17] F. R. Mayo, F. M. Lewis, Copolymerization. I. A basis for comparing the behavior of monomers in copolymerization; the copolymerization of styrene and methyl methacrylate, Journal of the American Chemical Society 66 (9) (1944) 1594–1601.